COBEM 2023 27TH INTERNATIONAL CONGRESS OF MECHANICAL ENGENEERING

ABCM Brazilian Society of Mechanical Sciences and Engineering
27th ABCM International Congress of Mechanical Engineering
December 04-08, 2023, Florianópolis-SC, Brazil

COB-2023-1352
ENERGETIC, EXERGETIC AND ECONOMIC ANALYSES OF A KALINA CYCLE DRIVEN BY SOLAR THERMAL ENERGY IN THE BOM JESUS DA LAPA-BA CITY

Géssica Silva Amorim
Juan Jose Garcia Pabon
Universidade Federal de Itajubá, Campus Prof. José Rodrigues Seabra, CEP 37500-093, Itajubá, Minas Gerais, Brasil.
d2022103017@unifei.edu.br
jjgp@unifei.edu.br

Andre Issao Sato
Universidade Federal do Oeste da Bahia, Centro Multidisciplinar de Bom Jesus da Lapa, CEP 47600-000, Bom Jesus da Lapa, Bahia, Brasil.
andre.sato@ufob.edu.br

Abstract. *The use of fossil fuels during the industrialization process in the last century has resulted in climate change, due to the large emissions of pollutants into the atmosphere, which are emerging points of debate in the current decade, as enacted in the Paris Plan and reported in the latest report of the Intergovernmental Panel on Climate Change (IPCC). There is a need to make the world's energy matrix based on renewable energy sources which, although attractive, are intermittent sources. In this study, parabolic trough solar concentrators are coupled to a Kalina cycle to study the system's performance throughout the year. Energy availability was based on solar irradiation data collected from the National Meteorological Institute (INMET) database for the Bom Jesus da Lapa-Ba municipality. Mathematical modeling was developed by applying mass, energy and exergy balances to each control volume. An economic analysis was then carried out to obtain the levelized cost of energy (LCOE) and payback (Pb) values. The results show that the cycle has an energy efficiency of 14% and an average exergy efficiency of 12.14%. In addition, the exergy analysis shows that the main source of energy destruction is the solar concentrators and the condenser. Finally, the LCOE of 0.41$/kWh and a payback of 4.5 years were obtained.*

Keywords: *Kalina cycle, computacional modeling, energy efficiency, exergy efficiency, economic analisys.*

1. INTRODUCTION

In the face of growing environmental concerns, the transition to a sustainable energy system brings a combination of new opportunities and challenges, which is enabling countries around the world to rapidly move away from carbon-emitting sources (IPCC, 2022). However, renewable energy has some limitations, including climatic and geographical factors that mean that some sources have low temperatures, such as industrial waste heat, geothermal energy and solar thermal energy. Therefore, conventional thermodynamic energy cycles have low heat-to-energy conversion rates, requiring some modifications for their applicability (Xia et al., 2019).

In 1983, Alexander Kalina presented the Kalina cycle (KCS) for the first time, which used a system for utilizing waste heat from a diesel cycle engine and a working fluid made up of a mixture of water and ammonia (Kalina, 1983). This cycle, which is been studied to actual day, is an improvement on the Rankine cycle that operates with a mixture of fluids, which allows for more efficient heat recovery by reducing irreversibility during the evaporation process. In addition, it has the ability to adapt to low, medium and high temperature sources, thus presenting various configurations for specific applications (Srinivas et al., 2019). Compared to high-temperature thermal energy storage, this system can reduce the design difficulty of the main system components and the equipment material requirements, improving the application feasibility (Y. Zhang et al., 2023).

The current literature is based on improving and optimizing the Kalina cycle. Masrur Hossain et al. (2021) explored the potential benefits and limitations of the proposed modifications in contrast to the KCS-34, by means of thermodynamic modeling and optimization. X. Zhang e Li (2022) proposed different redesigned cycles with a single-screw expander based on the Kalina Cycle System 11, 34 and 34g. Cheng et al. (2022) explored the dynamic behavior of the Kalina cycle system for operational safety due to fluctuating low-grade heat sources and external load. Kojur et al. (2023) performed a multi-objective optimization of the cycle using the particle swarm optimization algorithm. One of the studies using low-temperature solar energy associated with the Kalina cycle was proposed by Babaelahi, Mofidipour, e Rafat (2019) who presented a new method for designing and optimizing the Kalina plant powered by a linear parabolic trough solar collector.

Regarding as solar heat, parabolic trough collectors (PTC) are a suitable candidate for low to medium temperature Kalina cycles, playing a key role in harnessing solar energy efficiently and sustainably (Adun et al. 2021), (S. K. Singh et al., 2023). PTCs concentrate solar insolation on the focal axis of the parabolic reflectors where the receiver is located, and the absorber receives the thermal energy from the incoming solar radiation and transmits it to the heat transfer fluid (Shahzad Nazir et al., 2021).

On the Brazilian and world stage, Bahia has one of the best solar resources, ranking second in centralized generation in Brazil, in addition to the availability of areas, strategic location and favorable logistical infrastructure (Gil et al., 2023). In particular, the Bom Jesus da Lapa municipality, which occupies an area of 415,510 km² and has around 70,151 thousand inhabitants (IBGE, 2021) has more than 12 hours of sunshine a day and a temperature that is usually around 35 degrees. In 2017 it already produced 158 megawatts (MW) in its solar plants, with the great advantage of abundant land that doesn't compete with agribusiness (ABSOLAR, 2017).

Despite the valuable work carried out on the Kalina cycle application at low temperatures, some gaps have been observed on which further research should be carried out, including the feasibility of this system exploiting the potential for solar thermal energy in the state of Bahia. In this study, the Kalina cycle thermodynamic modeling powered by solar thermal energy was carried out from an energy, exergetic and economic view point. Firstly, the principle of mass conservation and the first law of thermodynamics were selected to evaluate the thermodynamic parameters. Next, the energy balance equation is applied to each thermodynamic state, and then irreversibility and energy efficiency are calculated for each component. Then, the system economic analysis is carried out using the levelized cost of electricity (LCOE) and the simple payback (Pb) as indicators.

2. METHODOLOGY

The object of study of this work consists of a system composed of two cycles: the subcycle of conversion of thermal energy into electrical energy, called the Kalina cycle, and a subcycle of solar thermal energy. Figure (1) illustrates a schematic diagram of the Kalina cycle driven by thermal solar energy.

The topics below present in detail the necessary steps for the developed calculations.

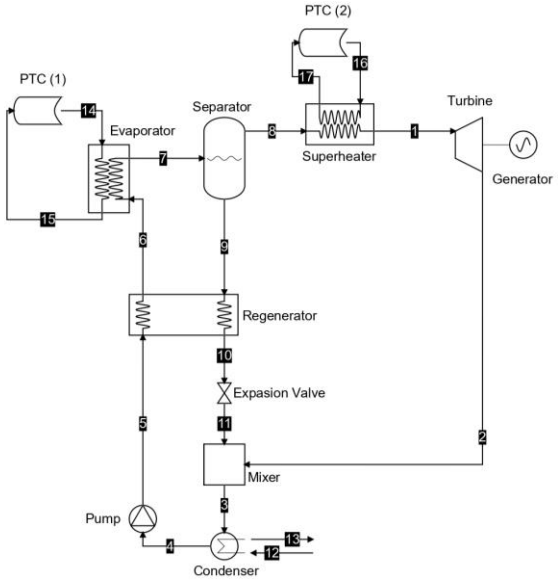

Figure 1. Off-grid system using the Kalina cycle driven by solar thermal energy.

2.1 System description

The Kalina cycle operates with an ammonia-water mixture. In the work production stage, the steam expands in the turbine (1) - (2), converting the thermal energy of the fluid into mechanical energy, and is then mixed with the ammonia-poor saturated liquid mixture (11) coming out of the separator. The mixture is then condensed (4) and pumped to the regenerator (5), whose fluid gains heat before entering the evaporator (6). The evaporator heats the fluid to a temperature between the dew point and the bubble point of the mixture and then the mixture of liquid and vapor phases is sent to the separator (7). The mixture is separated into ammonia-rich vapor (8) and ammonia-poor saturated liquid (9) using a density difference mechanism between the fluids. The ammonia-poor fluid loses heat (9) - (10) and is expanded (11) before entering the mixing chamber. The ammonia-rich fluid is superheated (8) - (1) before entering the turbine.

In this study, a parabolic trough concentrator (PTC) is integrated into the Kalina cycle, which operates by heating Therminol VP-1 oil.

2.2 Kalina Cycle mathematical model

In this study, some flow design assumptions were applied to simplify the analysis of the Kalina Cycle system. The system modeling therefore assumes:

- A steady state operation is assumed for the system;
- Negligible kinetic and potential energy variations in the components;
- Viscous effects along the system are negligible;
- Negligible pressure drop, except for: turbine, pump and expansion valve;
- Expansion valve operating isentalpic;
- Negligible heat loss to the environment, except solar concentrator;
- Isentropic efficiencies of the pump and turbine are considered constant;
- The upper and lower outlet stream of the separator is in saturated vapor and saturated liquid situation, respectively.

The application of thermodynamic principles in this case was based on Bejan (2016) and Kojur et al. (2023). According to the author, the mass flow in a control volume that has inlet and outlet regions at the system boundary is given by Eq. (1).

$$\sum_{in} \dot{m} = \sum_{out} \dot{m} \tag{1}$$

Where $\dot{m}$ is the mass flow rate.

In the absence of macroscopic forms of energy storage, except kinetic and gravitational, the terms that account for energy transfer via mass flow (Bejan, 2016) are given by Eq. (2).

$$\dot{Q} - \dot{W} = \sum_{out} \dot{m}\,(h + \frac{1}{2}V^2 + gz) - \sum_{in} \dot{m}\,(h + \frac{1}{2}V^2 + gz) \tag{2}$$

Where $\dot{Q}$ e $\dot{W}$ are the heat and mass transfer rates across the system boundary, respectively, and h, $\frac{1}{2}V^2$, gz are the enthalpy, kinetic energy, and gravitational energy, in that order.

For heat exchangers, the area can be defined using Eq. (3), which uses the logarithmic mean temperature difference (ΔT^{LMTD}) (Kojur et al., 2023).

$$\dot{Q} = UA\Delta T^{LMTD} \tag{3}$$

Where U is the overall heat transfer coefficient and A is the heat exchanger area.

The equation (4) Kojur et al. (2023) was used to determine the thermal efficiency (η_e) of the Kalina cycle:

$$\eta_e = \frac{\dot{W}_{turbine} - \dot{W}_{pump}}{\dot{Q}_{evap} + \dot{Q}_{sup}} \tag{4}$$

According to Bejan (2016), by combining the first law with the second law it is possible to observe that whenever a system operates irreversibly, it destroys work at a rate proportional to the system's entropy generation rate (S_{gen}).

$$S_{gen} = \sum_{out} \dot{m} \times s - \sum_{in} \dot{m} \times s - \sum_{k} \frac{\dot{Q}}{T_k} \tag{5}$$

Where s is the entropy and T_k the temperature reservoir.

The total flow exergy (e_{total}) is then defined from the sum of the thermomechanical ($e_{physical}$) and chemical ($e_{chemical}$) exergy contributions.

$$e_{total} = e_{physical} + e_{chemical} \tag{6}$$

Chemical exergy is calculated from the difference in chemical potential between the two states but is not considered for calculation purposes as it is applied to fuels (Kojur et al., 2023). Physical exergy is defined as the difference between the flow availability of the stream and that of the same stream in its restricted dead state, i.e., the flow availability evaluated under standard environmental conditions (T_0, P_0).

$$e_{physical} = (h - h_0) - T_0(s - s_0) \quad (7)$$

Thus, for a steady-state system, the exergy balance is defined by Eq. (8) (Bejan, 2016).

$$\dot{E}_{in} = \dot{E}_{out} + \dot{E}_D + \dot{E}_W + \dot{E}_Q \quad (8)$$

Where $\dot{E}_D$ is the exergy destruction rate, $\dot{E}_{\dot{W}}$ is the exergy rate associated with the work transfer, and $\dot{E}_Q$ is the exergy rate associated with the heat transfer.

The exergy efficiency for different components of the cycle is calculated by the ratio between the product exergy flow ($\dot{E}_P$) and the fuel exergy flow ($\dot{E}_F$), defined by Eq. (9) (Kojur et al., 2023).

$$\eta_{ex} = \frac{\dot{E}_P}{\dot{E}_F} \quad (9)$$

Quantitative thermodynamic analysis can be presented for these cycles by establishing the energy balance relationships between each component. Also, exergetic analysis can be applied to determine the potential work lost due to irreversibility in a specific dead state. According to Bejan (2016) the equations governing operation in steady state are simpler because the time derivatives disappear. Applying this analysis to the Kalina cycle presented, the governing equations for the mass, energy, and exergy balances can be obtained from Table 1.

Table 1. Mass, energy and exergy balance for the thermodynamic states of the Kalina cycle.

Components	**Mass balance**	**Energy balance**	**Exergy balance**
Evaporator	$\dot{m}_6 = \dot{m}_7$ $\dot{m}_{15} = \dot{m}_{16}$	$\dot{Q}_{evap} = \dot{m}_7(h_7 - h_6) = \dot{m}_{15}(h_{14} - h_{15})$	$\dot{E}_6 + \dot{E}_{14} = \dot{E}_7 + \dot{E}_{15} + \dot{E}_{D,evap}$
Condenser	$\dot{m}_3 = \dot{m}_4$ $\dot{m}_{12} = \dot{m}_{13}$	$\dot{Q}_{cond} = \dot{m}_3(h_3 - h_4) = \dot{m}_{12}(h_{13} - h_{12})$	$\dot{E}_3 + \dot{E}_{12} = \dot{E}_4 + \dot{E}_{13} + \dot{E}_{D,cond}$
Regenerator	$\dot{m}_9 = \dot{m}_{10}$ $\dot{m}_5 = \dot{m}_6$	$\dot{Q}_{reg} = \dot{m}_9(h_9 - h_{10}) = \dot{m}_5(h_6 - h_5)$	$\dot{E}_5 + \dot{E}_9 = \dot{E}_6 + \dot{E}_{10} + \dot{E}_{D,reg}$
Superheater	$\dot{m}_8 = \dot{m}_1$ $\dot{m}_{14} = \dot{m}_{15}$	$\dot{Q}_{sup} = \dot{m}_1(h_1 - h_8) = \dot{m}_{14}(h_{16} - h_{17})$	$\dot{E}_8 + \dot{E}_{16} = \dot{E}_1 + \dot{E}_{17} + \dot{E}_{D,sup}$
Mixer	$\dot{m}_2 + \dot{m}_{11} = \dot{m}_3$	$h_2\dot{m}_2 + h_{11}\dot{m}_{11} = h_3\dot{m}_3$	$\dot{E}_2 + \dot{E}_{11} = \dot{E}_3 + \dot{E}_{D,mixer}$
Turbine	$\dot{m}_1 = \dot{m}_2$	$\dot{W}_{turb} = \dot{m}_1(h_1 - h_2)$	$\dot{E}_1 = \dot{E}_2 + \dot{W}_{turb} + \dot{E}_{D,turb}$
Pump	$\dot{m}_4 = \dot{m}_5$	$\dot{W}_{pump} = \dot{m}_4(h_5 - h_4)$	$\dot{E}_4 + \dot{W}_{pump} = \dot{E}_5 + \dot{E}_{D,pump}$
Expansion Valve	$\dot{m}_{10} = \dot{m}_{11}$	$h_{10}\dot{m}_{10} = h_{11}\dot{m}_{11}$	$\dot{E}_{10} = \dot{E}_{11} + \dot{E}_{D,valve}$
Separator	$\dot{m}_8 + \dot{m}_9 = \dot{m}_7$	$h_8\dot{m}_8 + h_9\dot{m}_9 = h_7\dot{m}_7$	$\dot{E}_7 = \dot{E}_8 + \dot{E}_9 + \dot{E}_{D,separator}$

The necessary boundary conditions used in the computer simulation of the Kalina cycle are listed in Table 2.

Table 2. Operating parameters of the Kalina cycle.

Description	**Parameter**	**Value**	**Unit**	**Reference**
Environment	T_0	298.15	K	(International System of Units)
	P_0	101.32	kPa	
Condenser	T_{12}	298.15	K	(Kojur et al., 2023)
	T_{13}	308.15	K	
Evaporator	P_6	4000.0	kPa	(O. K. Singh & Kaushik, 2013)
	T_{14}	403.15	K	(Srinivas et al., 2019)
Superheater	T_{16}	473,15	K	(Srinivas et al., 2019)
Pinch Point	PP	5	K	(Horta et al., 2021)
Turbine	$\eta_{isen,turbine}$	85	%	
Pump	$\eta_{isen,pump}$	85	%	
Heat transfer coefficient	U_{sup}	600	W/m² K	(Köse et al., 2022)
	U_{evap}	900		(Campos Rodríguez et al., 2013)
	U_{cond}	1100		
	U_{reg}	1000		

Then, the following parameters are introduced to investigate the cycle's performance. The exergetic efficiency of the Kalina cycle can then be defined using Eq. (10).

$$\eta_{ex} = \frac{\dot{W}_{turbine} - \dot{W}_{pump}}{\dot{E}_{D,PTC}} \tag{10}$$

Where $\dot{E}_{D,PTC}$ corresponds to irreversibilities in parabolic trough solar concentrators.

2.3 Mathematical model of the thermal solar energy cycle

According to Kalogirou et al. (2016), parabolic trough solar concentrators are currently the most mature technology for solar thermal electricity conversion due to their ability to operate at higher temperatures (up to 400 °C), thus having the potential to achieve higher thermal efficiencies. The useful heat gain (Q_u) and concentrator efficiency (η_{PTC}) are determined using Eq. (11) e (12), respectively (Desai & Bandyopadhyay, 2015).

$$Q_u = m_f(h_{out} - h_{in}) = \eta_{PTC} \times I \times A_{PTC} \tag{11}$$

$$\eta_{PTC} = \eta_o - \frac{U_l(T_a - T_0)}{I} \tag{12}$$

Where A_{PTC} is the aperture area, η_o is the optical efficiency and U_l is the heat loss coefficient based on the aperture area of the concentrator field, m_f is the mass flow rate of the working fluid, T_a is the average temperature of the working fluid that entering and leaving the concentrator and I is the direct normal irradiance.

Eventually, the sum of the losses and the exergy of destruction in the concentrator is calculated from the difference between the fuel exergy and the product exergy. The exergy balance in the PTC's is then defined using Eq. (13) (Babaelahi et al., 2019).

$$\dot{E}_{16} + \dot{E}_{sun} = \dot{E}_{14} + \dot{E}_{D,PTC} \tag{13}$$

So, the exergy from the sun can be determined from Eq. (14) (Kalogirou et al., 2016).

$$\dot{E}_{sun} = I \times A_{PTC} \times \left(1 + \frac{1}{3}\left(\frac{T_0}{T_S}\right)^4 - \frac{4}{3}\left(\frac{T_0}{T_S}\right)\right) \tag{14}$$

Where T_S is the equivalent temperature of the sun in Kelvin. The values used for this analysis is calculated based on data in Table 3.

Table 3. Parabolic trough solar concentrator characteristics.

Input parameter	Value/Type	Reference
Concentrator model	Parabolic Trough Concentrator (PTC)	(Desai & Bandyopadhyay, 2015)
Heat transfer fluid	Therminol VP-1	
Optical efficiency	$\eta_o = 0.7$	
Heat loss coefficient	$U_l = 0.1$ W/(m^2.K)	
Sun temperature	$T_s = 5570$ K	(Kojur et al., 2023)

2.4 Economic analysis

The economic model is considered in this study to calculate the levelized cost of electricity generated (LCOE) and the payback time. The cost estimation method used in this work was based on Köse et al. (2022) and Ashouri et al. (2015).

In this case, the LCOE was calculated considering only the cost relating to installation, operation, and maintenance, since solar energy was considered to have zero cost. Equation (15) describes the electricity cost generated in $/kWh.

$$LCOE = \frac{c_{invest}\left(\frac{IF_{ref}}{IF_{actual}}\right)crf + c_{O\&M} + c_{fuel}}{Energy_{year}} \tag{15}$$

Where $Energy_{year}$ is yearly energy production, c_{invest} is the investment costs, crf to capital recovery factor, IF_{ref} e IF_{actual} to the reference and current indexation indexes, respectively, Hr operating hours number per year and $c_{O\&M}$ and c_{fuel} the operation and maintenance and fuel costs, respectively.

The investment cost comprises the sum of the costs of each equipment, which is determined by the equations in Table 4. Here, the cost of the equipment purchased for the mixing chamber is not considered due to its low cost.

Table 4. Capital cost of components.

Components	Capital Cost	Reference
Evaporator	$C_{eva} = 1397 * A_{eva}^{0,89}$	(Köse et al., 2022)
Condenser	$C_{cond} = 1397 * A_{cond}^{0,89}$	
Superheater	$C_{sup} = 1397 * A_{sup}^{0,89}$	
Regenerator	$C_{reg} = 2681 * A_{reg}^{0,59}$	
Pump	$C_{pump} = 1120 * \dot{W}_{pump}^{0,8}$	
Turbine	$C_{turb} = 4405 * \dot{W}_{turb}^{0,7}$	
Separator	$C_{sep} = 280{,}3 * \dot{m}_{sep}^{0,67}$	
Concentrator	$C_{PTC} = 150 * A_{PTC}$	(Y. Zhang, Ma, et al. 2023)

The capital recovery factor is determined using the long-term interest rate (i) and the number of years of useful life (n), given by Eq. (16).

$$crf = \frac{i(1+i)^n}{(1+i)^n - 1} \tag{16}$$

After calculating the levelized cost of electricity, the plant's simple payback time can be calculated using Eq. (17) as a function of the cost of electricity ($c_{electricity}$).

$$Pb = \frac{c_{total}}{\dot{W}_{liquid} \times Hr \times c_{\text{electricity}}} \tag{17}$$

The simulation conditions for the system economic analysis are given in Table 5.

Table 5. Economic constraints.

Description	Parameter	Value	Reference
Useful life	n	20 years	(Köse et al., 2022)
Interest rate	i	13.75%	-
Operation and maintenance costs	$c_{O\&M}$	$0.06 \times c_{invest}$	(Bejan, 2016)
Reference indexation index	IF_{ref}	120	(BOE, 2022)
Current indexation index	IF_{atual}	100	
Cost of electricity sale	$c_{electricity}$	0.45 $/kWh	-

3. RESULTS AND DISCUSSIONS

3.1 Validation of the model

In this section, the temperature, pressure, enthalpy, and entropy of the different points of the Kalina cycle obtained in this study are compared with the simulation values of Kojur et al. (2023) to validate the results. Table 6 shows the results obtained in the two studies, based on Figure 1, whose cycle operates without a superheater and, consequently, states 8, 16 and 17 are non-existent.

The model fits with good agreement, however, the entropy values for state 1 showed a large divergence. Although, this characteristic did not significantly affect the cycle's output parameters.

Table 6. Comparison of the mathematical model of the Kalina cycle.

State	T (K)	T (K)[1]	P (kPa)	P (kPa)[1]	h (kJ/kg)	h (kJ/kg)[1]	s (kJ/kg K)	s (kJ/kg K)[1]
1	423,15	423,15	3000	3000	1684	1688	4.919	3.931
2	371,07	371,20	800.0	800.0	1505	1508	5.040	5.052
3	362,00	362,30	800.0	800.0	997.4	1006	3.554	3.582
4	304,35	303,90	800.0	800.0	-49.97	-51.98	0.3561	0.349
5	304,82	304,40	3000	3000	-46.14	-48.26	0.3586	0.351
6	340,69	339,90	3000	3000	123.5	119.5	0.884	0.873
7	423,15	423,15	3000	3000	1288	1295	3.916	3.937
9	423,15	423,15	3000	3000	473.9	474.4	1.858	1.859
10	309,82	309,40	3000	3000	-43.58	-44.38	0.4408	0.436
11	310,27	309,40	800.0	800.0	-43.58	-44.38	0.4489	0.444
12	298,15	298,15	101.3	101.3	-	-	-	-
13	308,15	308,15	101.3	101.3	-	-	-	-

[1] (Kojur et al., 2023)

3.2 Computational model and parametric analysis

For the thermodynamic modeling of the Kalina cycle and the solar concentrators, the energy and mass equations described in Table 1 and the input values in Table 2 are used to obtain the output values for temperature, pressure, enthalpy, entropy, mass flow, ammonia mass fraction (x) and titer (q) of the different thermodynamic states of the cycle. Table 7 shows the thermodynamic states for radiation and ambient temperature of 705.9 W/m² and 25ºC, respectively.

Table 7. Thermodynamic properties of the cycle operating with radiation of 705.9 W/m² and a temperature of 25ºC.

State	T (ºC)	P (kPa)	h (kJ/kg)	s (kJ/kg K)	x (kg/kg)	q	$\dot{m}$ (kg/s)
1	468,15	4000	1698	4.819	0.973	V.S.[1]	0.98
2	341,74	687.1	1434	4.957	0.973	0.99	0.98
3	317,38	687.1	323.4	1.594	0.6577	0.26	3.70
4	303,15	687.1	-73.54	0.318	0.6577	0	3.70
5	303,72	4000	-68.40	0.320	0.6577	L.C.[2]	3.70
6	367,23	4000	235.2	1.226	0.6577	L.C.	3.70
7	395,15	4000	636.5	2.269	0.6577	0.26	3.70
8	395,15	4000	1470	4.298	0.973	1	0.98
9	395,15	4000	337.9	1.542	0.5448	0	2.72
10	308,72	4000	-74.40	0.368	0.5448	L.C.	2.72
11	309,31	687.1	-74.40	0.382	0.5448	L.C.	2.72
12	298,15	101.3	104.8	0.367	-	-	35.1
13	308,15	101.3	146.7	0.505	-	-	35.1
14	403,15	-	-	1.668	-	-	18.6
15	372,23	-	-	1.468	-	-	18.6
16	473,15	-	-	1.932	-	-	1.13
17	403,15	-	-	1.590	-	-	1.13

[1] superheated steam, [2] compressed liquid.

Using the exergy equations described in Table 1 and Eq. (13) and (14), it was possible to determine the exergies of the flows corresponding to the products and fuels, as well as the irreversibilities in each component of the Kalina cycle and solar energy sub-cycle. Table 8 quantifies the cycle's heat and power rates, as well as the exergetic efficiencies of the main components, under the same operating conditions as in Table 7.

It can be seen from the values obtained that the greatest destruction of exergy occurs in the solar concentrators. This is due to a large temperature difference between input and output flows. Therefore, a careful collector design is necessary to decrease the losses. In the Kalina cycle, the components with the greatest exergy destruction were the condenser and regenerator. Otherwise, the exergetic efficiency is higher for the turbine and pump. In this case, the net power, irreversibilities and energy and exergy efficiencies of the cycle correspond to 238.8 kW, 2086 kW, 14% and 13%, respectively.

Table 8. Heat, power and irreversibilities of the cycle.

Components	$\dot{Q}$ **ou** $\dot{W}$ **(kW)**	$\dot{E}_P$ (kW)	$\dot{E}_F$ (kW)	$\dot{E}_D$ (kW)	η_{ex} **(%)**
Solar concentrator	1708	4856	2311	1825	21.03
Evaporator	1485	335	378	44	88.47
Superheater	223	71	1768	37	4.02
Turbine	258	258	298	40	86.57
Regenerator	1123	124	170	46	72.83
Condenser	1469	24	61	37	39.68
Pump	19	16	19	3	85.29

The effects of some of the input parameters on the cycle's energy and exergy efficiency were also analyzed. With the same operating conditions as in Table 7, Figure (2) shows the analysis of the effect of the ammonia mass fraction in the working fluid at different maximum cycle pressures.

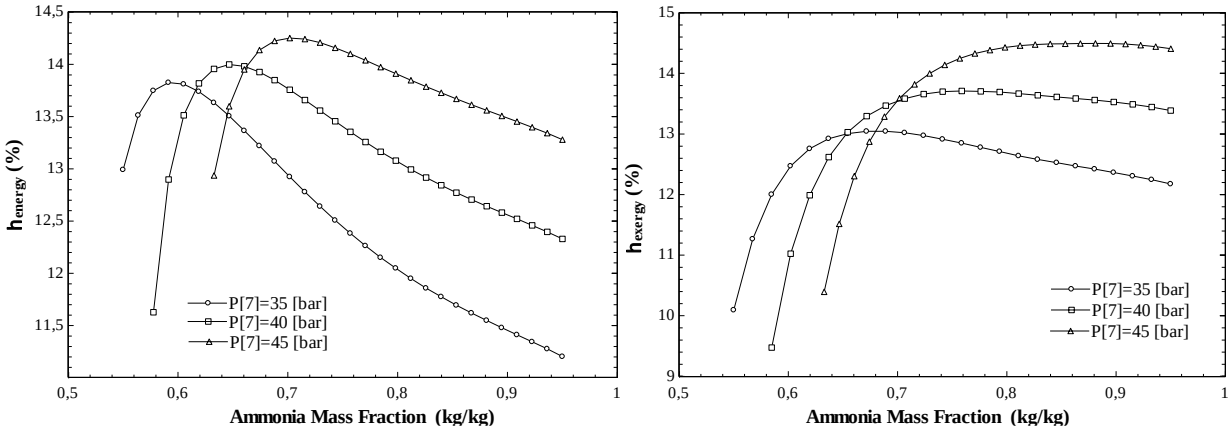

(a) (b)

Figure 2. Effect of varying the ammonia mass fraction on: (a) the energy efficiency and (b) the exergetic efficiency of the cycle.

In Figure (2) (a) we see that for each pressure there is a certain ammonia mass fraction whose cycle reaches its maximum thermal efficiency. This happens because the ammonia specific heat capacity is lower than that of water, so the steam flow produced in the evaporator increases and then the mass flow rate in the turbine increases. Parallel to this, the increase in the ammonia mass fraction at the turbine inlet results in a decrease in the enthalpy difference between the ammonia and water. Thus, after reaching its maximum point, the increase in the mass flow rate in the turbine does not compensate for the decrease in the enthalpy difference between the ammonia and the water in the turbine, causing a decrease in the cycle efficiency. On the other hand, Figure (2) (b) shows that the exergy efficiency curves tend to remain constant at higher pressures and ammonia mass fractions. The reason may be that for low values of ammonia mass fraction, the irreversibility of the turbine is high due to higher entropy generation, resulting in low second law efficiency. And the entropy generation becomes smaller at higher pressures.

3.3 Energy production

The climate data for temperature and radiation was summarized into a typical day for each month and then the model was used for the 288 temperature and radiation data, which Figure 3 illustrates.

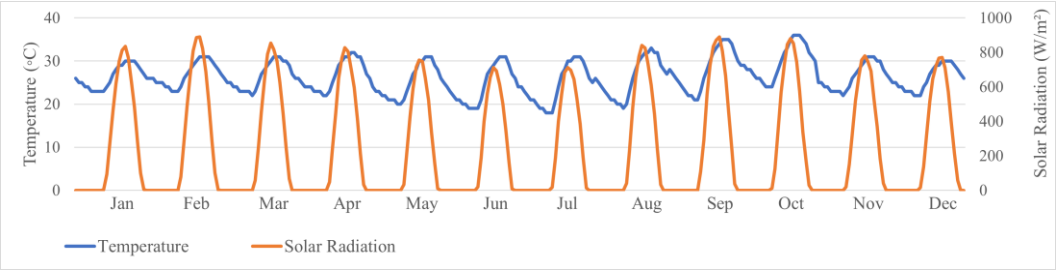

Figure 3. Variation in temperature and radiation for the average day of each month during the year.

The monthly energy produced by the proposed system was calculated, as shown in Figure 4. The annual amount corresponds to 712.9 MWh.

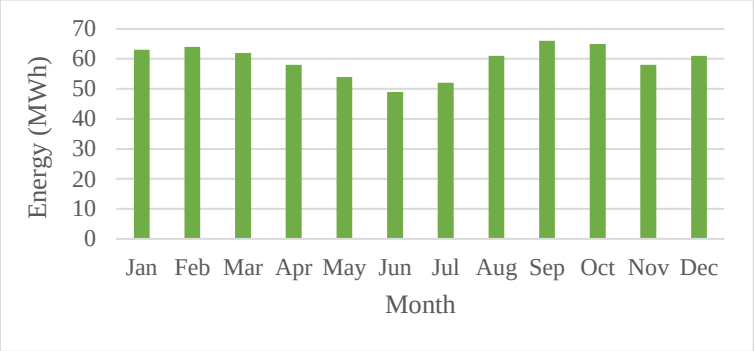

Figura 4. Energy generation potential for each month of the year.

3.4 Economic analysis

In terms of initial investment, the turbine and evaporator account for a large part of the Kalina cycle total cost, around 61.9% in this case. The cost of the PTC power station was $528637. According to Eq. (16), the LCOE is a function of the initial investment, the operation and maintenance cost and the fuel. However, the solar energy cost is equivalent to zero. Compared to other Kalina cycle studies, the LCOE of the proposed system (0.41 $/kWh) and the payback (4.5 years) are lower than in the reference literature of 0.43 $/kWh and 6 years, respectively (Ashouri et al., 2015). This fact was expected mainly due to the difference in time in which the reference work was developed.

Table 9 shows the capital costs for each component of the Kalina cycle.

Table 9. Capital costs for each equipment.

Component	**Cost (*USD*)**
Turbine	214764
Evaporator	196014
Condenser	151476
Superheater	51933
Regenerator	36686
Pump	11829
Separator	673

4. CONCLUSION

This work was carried out to thermodynamically and economically evaluate the Kalina cycle used to provide power with parabolic trough concentrators as a heat source. Eventually, some results were noted with the development of this study:

- Operating at an average direct solar radiation of 705.9 W/m², with an ammonia mass fraction of 0.66 kg/kg in the evaporator, and a maximum pressure and temperature of 4 MPa and 200 ºC, respectively, the cycle showed an energy efficiency of 14% and an exergy efficiency of 13.09%, generating 238.8 kW of net power;
- The maximum efficiency of the cycle was calculated by means of parametric analysis of the ammonia mass fraction and maximum pressure leaving the concentrator for the evaporator;
- The highest rate of exergy destruction occurs in the solar concentrators and condenser. The turbine, which is the most expensive piece of equipment in the system, accounts for 13,4% of the exergy destroyed;
- The average exergy efficiency of 12.14%, and the yearly energy produced is 712.9 MWh;
- For the proposed system, the LCOE and payback were equivalent to approximately 0.41 $/kWh and 4.5 years, respectively.

5. ACKNOWLEDGEMENTS

The authors would like to thank FAPEMIG for granting a master's scholarship to author Géssica Silva Amorim and CAPES and CNPQ for their financial support.

6. REFERENCES

ABSOLAR, 2017. *A cidade de Bom Jesus da Lapa vira a Capital brasileira da energia solar*. https://www.absolar.org.br/noticia/a-cidade-de-bom-jesus-da-lapa-vira-a-capital-brasileira-da-energia-solar/

Ashouri, M., Khoshkar Vandani, A. M., Mehrpooya, M., Ahmadi, M. H., & Abdollahpour, A., 2015. *Techno-economic assessment of a Kalina cycle driven by a parabolic Trough solar collector*. Energy Conversion and Management, 105, 1328–1339.

Babaelahi, M., Mofidipour, E., & Rafat, E., 2019. *Design, dynamic analysis and control-based exergetic optimization for solar-driven Kalina power plant*. Energy, 187, 115977.

Bejan, Adrian., 2016. *Advanced engineering thermodynamics*. Wiley.

BOE, C. S. B. of E., 2022. *Equipment and Fixtures Index, Percent Good and Valuation Factors*. https://www.boe.ca.gov/proptaxes/pdf/ah58121.pdf

Campos Rodríguez, C. E., Escobar Palacio, J. C., Venturini, O. J., Silva Lora, E. E., Cobas, V. M., Marques Dos Santos, D., Lofrano Dotto, F. R., & Gialluca, V., 2013. *Exergetic and economic comparison of ORC and Kalina cycle for low temperature enhanced geothermal system in Brazil*. Applied Thermal Engineering, 52(1), 109–119.

Cheng, Z., Wang, J., Yang, P., Wang, Y., Chen, G., Zhao, P., & Dai, Y., 2022. *Comparison of control strategies and dynamic behaviour analysis of a Kalina cycle driven by a low-grade heat source*. Energy, 242, 122958.

Desai, N. B., & Bandyopadhyay, S., 2015. *Optimization of concentrating solar thermal power plant based on parabolic trough collector*. Journal of Cleaner Production, 89, 262–271.

Gil, S. G., Sauaia, R., & Koloszuk, R., 2023. *O que é que a Bahia tem? Tem potencial solar como ninguém!* ABSOLAR. https://www.absolar.org.br/artigos/o-que-e-que-a-bahia-tem-tem-potencial-solar-como-ninguem/

Horta, G. R. da C., Barbosa, E. P., Moreira, L. F., Arrieta, F. R. P., & Oliveira, R. N. de., 2021. *Comparison of Kalina cycles for heat recovery application in cement industry*. Applied Thermal Engineering, 195, 117167.

IBGE., 2021. Instituto Brasileiro de Geografia e Estatística.

IPCC, I. P. on C. C., 2022. *Climate Change 2022: Impacts, Adaptation and Vulnerability*. In Cambridge University Press. https://www.ipcc.ch/report/ar6/wg2/

Kalina, A. I., 1983. *Combined Cycle and Waste Heat Recovery Power Systems Based on a Novel Thermodynamic Energy Cycle Utilizing Low-Temperature Heat for Power Generation*.

Kalogirou, S. A., Karellas, S., Braimakis, K., Stanciu, C., & Badescu, V., 2016. *Exergy analysis of solar thermal collectors and processes*. Progress in Energy and Combustion Science, 56, 106–137.

Kojur, N. B., Namdar, M., Nasero, M. J., Aminian, S., Koosha, N., & Zarei, K., 2023. *Energy, exergy, economic, and exergoeconomic analyses and optimization of a solar Kalina cycle using particle swarm optimization algorithm*. Energy Conversion and Management: X, 100372.

Köse, Ö., Koç, Y., & Yağlı, H.2, 2022. *Is Kalina cycle or organic Rankine cycle for industrial waste heat recovery applications? A detailed performance, economic and environment based comprehensive analysis*. Process Safety and Environmental Protection, 163, 421–437.

Masrur Hossain, M., Afnan Ahmed, N., Abid Shahriyar, M., Monjurul Ehsan, M., Riaz, F., Salehin, S., & Awais Salman, C., 2021. *Analysis and optimization of a modified Kalina cycle system for low-grade heat utilization*. Energy Conversion and Management: X, 12, 100121.

Shahzad Nazir, M., Shahsavar, A., Afrand, M., Arıcı, M., Nižetić, S., Ma, Z., & Öztop, H. F., 2021. *A comprehensive review of parabolic trough solar collectors equipped with turbulators and numerical evaluation of hydrothermal performance of a novel model*. Sustainable Energy Technologies and Assessments, 45, 101103.

Singh, O. K., & Kaushik, S. C., 2013. *Energy and exergy analysis and optimization of Kalina cycle coupled with a coal fired steam power plant*. Applied Thermal Engineering, 51(1–2), 787–800.

Singh, S. K., Tiwari, A. K., & Paliwal, H. K., 2023. *Thermo-economic assessment of hybrid Kalina cycle and organic Rankine cycle system using a parabolic trough collector solar field*. Thermal Science and Engineering Progress, 46, 102132

Srinivas, T., Ganesh, N. S., & Shankar, R., 2019. *Flexible Kalina Cycle Systems*. Apple Academic Press.

Xia, L., Liu, R., Zeng, Y., Zhou, P., Liu, J., Cao, X., & Xiang, S., 2019. *A review of low-temperature heat recovery technologies for industry processes*. Chinese Journal of Chemical Engineering, 27(10), 2227–2237.

Zhang, X., & Li, Z., 2022. *Performance of Kalina cycle with single-screw expander for low-temperature geothermal energy utilizatio*n. Applied Thermal Engineering, 210, 118364.

Zhang, Y., Lin, F., Liu, Z., Lin, Y., & Yang, K., 2023. *Energy and exergy performance evaluation of a novel low-temperature physical energy storage system consisting of compressed CO2 energy storage and Kalina cycle*. Journal of Energy Storage, 60.

7. RESPONSIBILITY NOTICE

The authors are the only responsible for the printed material included in this paper.